

Sensitivity Analysis of One-port Characterized Devices in Vector Network Analyzer Calibrations: *Theory and Computational Analysis*

White Paper

Abstract

In this paper we present the results of a study on the use of characterized devices in microwave vector network analyzer (VNA) calibrations and measurements. We give a brief review of the theory of one-port characterized device calibration. One-port characterized devices such as coaxial opens, shorts and loads are attractive because of their ease of handling and their ruggedness as compared to more fragile devices like sliding loads. The scattering parameter error box representation and widely used terminology of error terms in one-port VNA calibrations such as directivity, source match and tracking are adopted in this paper. Based on these parameters, we examine the quality of one class of one-port VNA calibrations achievable through the use of characterized devices and the effects of different kinds of errors in device characterization can have on VNA calibrations. Computational analysis has revealed interesting properties of this class of calibrations that can lead to significant improvements in the accuracy of VNA measurements.

Speaker/Author: Godfrey Kwan
Agilent Technologies
2002 NCSL International Workshop & Symposium

Introduction

Error correction techniques in two-port environment have been proposed^[1,2] and used in industry for some time. In a model where the non-ideal behavior of a Vector Network Analyzer (VNA) is assumed to be separable from its ideal characteristics, it is widely accepted that a VNA can be described as a cascade of ideal reflectometers and error boxes. The error boxes are subsequently modeled by the theory of scattering parameters. This is a much simplified picture compared to the complexity of the architecture of modern VNAs. However, this simple model has been very successful in explaining the error correction mechanism of a VNA.

The procedure of characterizing the error boxes through the use of known devices is called network analyzer calibration. In a VNA configuration where there is only one port to be calibrated, as shown in Figure 1, the normalized components of this error box are known as directivity (D), source match (M) and tracking (T). These are three of the four 2-port S parameters of an error box, the fourth parameter has been normalized to unity. Γ_m is the reflection coefficient of the device under test modified by the error box. The test port reference plane P in Figure 1 is the plane separating the device under test and the test port of the VNA. Although we also assigned a second reference plane Q to the second port of the 2-port error box, this reference plane is only fictitious just as the 2-port error box itself.



In practice, one may determine the quantities D , M and T by connecting devices of known impedance to a particular test port and measuring each of these devices. These devices are calibration standards and will be referred to as characterized devices in this paper. This VNA calibration technique is known as Characterized Devices Calibration.

In cases where the device geometry and structure are simple enough, the device impedance can be calculated from measured physical dimensions and a few electrical parameters such as conductivity and dielectric constant. Device impedances can also be measured by a system that is of a high order of accuracy. In this paper, we will not be concerned with which of the above methods is actually used nor their relative merits. In any case, impedances of characterized devices can *never* be determined exactly. Slight errors in these “known” impedance values will lead to slight errors in the determination of the D , M and T values. It is the purpose of the present study to look into how these errors in the models of characterized devices can affect the accuracy in the determination of the error box and thus the uncertainties associated with scattering parameters measurements when using a VNA calibrated with such characterized devices.

In Figure 1, quantities D , M and T are sometimes called the raw error terms. And we shall refer to the error box bearing these 3 terms as the raw error box. The purpose of a calibration procedure is to determine these error terms. When a calibration is completed and the raw error terms are calculated, any future measurement done on the system can be corrected by making use of these error terms.

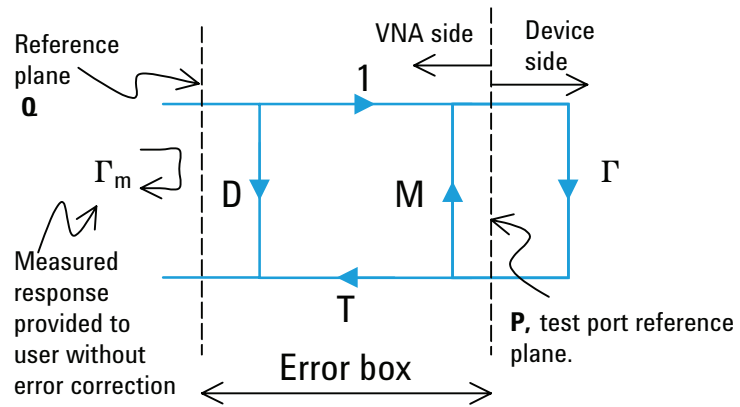


Figure 1. A test port modeled by an error box, a 2-port network of scattering parameters D , M and T . A one-port device of reflection coefficient Γ is connected to the test port.

One-Port Calibration Theory

After error correction is applied to a VNA measurement, the VNA is now operating in error *correction mode*. A VNA operated in such a manner can be further modeled by a similar signal flow graph as shown in Figure 2 where the D, M and T terms of the raw error box are now replaced by their respective residual errors. The original error box now becomes the residual error box. This error-corrected system, hybrid in nature, now consists of all the circuit components that make up the entire VNA, as well as the 2-port S-parameter error model that we have found to correct for any systematic error in the physical measurement. Measurement data provided under such circumstances are processed data and should be treated as such. In other words, these data are the result of a measurement plus an error term previously determined by a calibration procedure that may or may not be independent of the present measurement. The value of the error term may be related to the device that we are measuring. Even though this is not at all desirable, sometimes it is unavoidable.

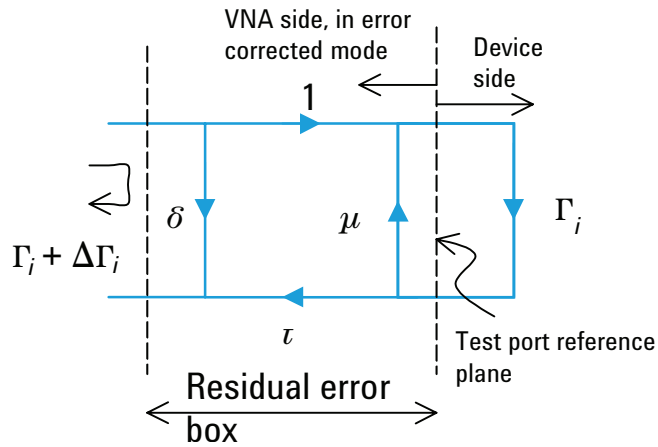


Figure 2. Residual error box description of a Vector Network Analyzer operating in error correction mode.

The residuals of the error box, residual directivity (δ), residual source match (μ) and residual tracking (τ), can be found in terms of errors in the reflection coefficients of the characterized devices^[3,4]. When a characterized device is connected to the test port shown in Figure 2, one obtains the following relationship:

$$\delta + \frac{\tau\Gamma_i}{1 - \mu\Gamma_i} = \Gamma_i + \Delta\Gamma_i; \quad i = 1,2,3. \quad (1)$$

where $\Gamma_i, i = 1,2,3$, are the actual reflection coefficients of the characterized devices and $\Delta\Gamma_i, i = 1,2,3$ are the errors in each of the reflection coefficients due to limitations in the models. This relationship can be re-arranged in the form of

$$1 \cdot \delta + \Gamma_i(\tau - \delta\mu) + \Gamma_i(\Gamma_i + \Delta\Gamma_i)\mu = \Gamma_i + \Delta\Gamma_i; i = 1,2,3. \quad (2)$$

and the residuals can be found exactly by solving this system of 3 equations in 3 unknowns. In matrix form, it can be conveniently expressed as follows:

$$\begin{bmatrix} \delta \\ \tau - \delta\mu \\ \mu \end{bmatrix} = \begin{bmatrix} 1 & \Gamma_1 & \Gamma_1(\Gamma_1 + \Delta\Gamma_1) \\ 1 & \Gamma_2 & \Gamma_2(\Gamma_2 + \Delta\Gamma_2) \\ 1 & \Gamma_3 & \Gamma_3(\Gamma_3 + \Delta\Gamma_3) \end{bmatrix}^{-1} \begin{bmatrix} \Gamma_1 + \Delta\Gamma_1 \\ \Gamma_2 + \Delta\Gamma_2 \\ \Gamma_3 + \Delta\Gamma_3 \end{bmatrix} \quad (3)$$

In theory, reflection coefficients of the three characterized devices need only be distinct and can be chosen to be any *arbitrary* value. However, we see from equation (3) that residuals of directivity, source match and tracking are functions of the errors in the reflection coefficients $\Delta\Gamma_i$'s of the three characterized devices as well as being functions of the reflection coefficients Γ_i 's themselves. It can be seen that for different reflection coefficients of the characterized devices, the residuals of directivity, source match and tracking take on a different functional dependence on the $\Delta\Gamma_i$'s. This is true even if the $\Delta\Gamma_i$'s remain constant when Γ_i 's vary. By carefully choosing one set of values that the reflection coefficients may take even when we have no control of their associated errors, we can still expect to minimize the values of the residuals to a certain extent.

Computational Analysis

Given the values of Γ_i 's and $\Delta\Gamma_i$'s, equation (3) can be used to compute the values of the residual errors. In the following case studies, nominal values of reflection coefficients for three characterized devices are selected. An error vector $\Delta\Gamma_i$ is added to the nominal reflection coefficient Γ_i . The sum of the nominal vector and the error vector, $\Gamma_i + \Delta\Gamma_i$, is the data vector provided by model data for a characterized device. By changing the magnitude and phase of the error vector, we can simulate the effects of errors in model data on the residuals. In this study, the magnitude and phase of the error vector are changed in such a way that the tip of the error vector takes on values inside a circular region at a total of 16 points. These points are approximately equally spaced from one another, clustered around the point Γ_i .

Parameters used in simulation are chosen to be typical for 2.4 mm precision slotless coaxial devices. That is, the error magnitudes we will be using are values we usually encounter in 2.4 mm coaxial devices. However, the errors in the models of shorts and opens are expressed in terms of degrees which makes the charts created in this study applicable for a wide range of frequencies and connector styles.

In practice, we usually characterize a matched load, an open and a short. This configuration of devices translates to $\Gamma_1 = 0$, $\Gamma_2 = 1$, $\Gamma_3 = -1$ in the ideal case. And it is this special case we will be studying in Case I to Case IV presented in this section.

In all figures, the following abbreviations and symbols are used.

$\Gamma_L, \Gamma_S, \Gamma_O$:	Reflection coefficient of load, short and open respectively.
$\text{Mag}(\Gamma_L)$:	Magnitude of reflection coefficient of load. Magnitudes of short and open are defined similarly.
$\text{Pha}(\Gamma_L)$:	Phase of reflection coefficient of load. Phases of short and open are defined similarly.
$\max(\Delta\Gamma_L)$:	Maximum value of amplitude of error vector of load. Quantities related to short and open are defined similarly.

Figure 3 illustrates Case Study I. The load error in this case is fixed. That is the error vector in the load is fixed and not swept at all while the errors in the open and the short are allowed to take on a number of values. This is done in order to illustrate how the curves in the simulation are generated and superimposed on one another. In this case, the error vector in the short model takes on only 20 values. Each curve in the graph corresponds to one value of the error vector in the short model. Although the error vector in the open model also takes on discrete values, we have plotted a continuous curve going through those points in order to produce a visual effect of a region of values that the residual source match can take. As more error vectors are allowed to sweep, the number of curves increases, effectively covering the whole region where data points are located. These regions of residual source match values are shown in another case study in Figure 4.

Case I

A fixed value, $\Gamma_L = 0.032$, is chosen for the load model. For the short and open, $\Gamma_s = -1$ and $\Gamma_o = 1$. The magnitudes of open and short models are fixed while their phases are varied between -0.5 to 0.5 . We assigned a nominal value of zero to the true value of the phase of open. And the phase of the short is assigned a value of 180 degrees. Twenty values between -0.5 and $+0.5$ are sampled with equal intervals.

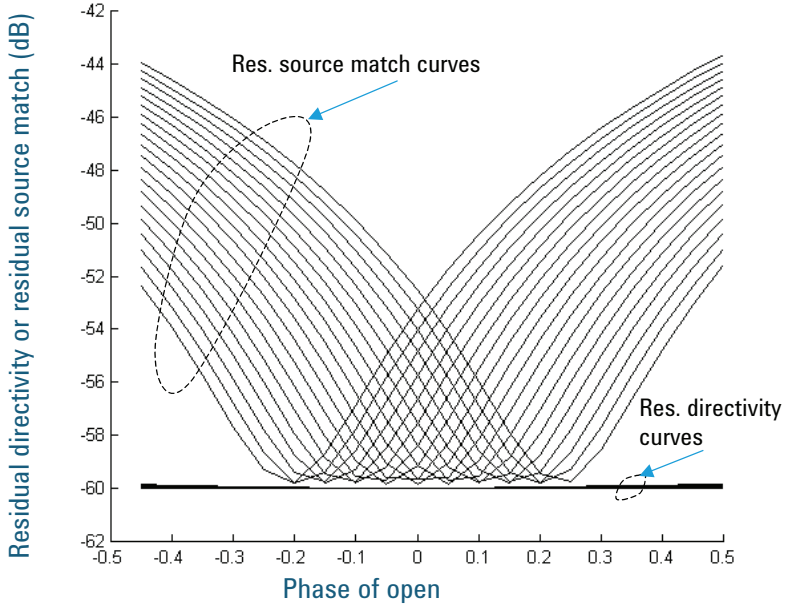


Figure 3. Curves of residual directivity and source match generated by sampling the complex plane of residual directivity and source match which are functions of 6 complex variables. It is a projection of the magnitudes of these residual functions onto the axis of the phase of the open model.

Case II: Full Sweep of All Three Errors in the Models.

In this case, the errors are fully swept for all three models of the characterized devices. In addition to that, 4 different percentage factors are used in order to show how the residual source match will change with increasing accuracy of the models. Errors are swept for 25%, 50%, 75% and 100% of their assigned maximum values. In the example shown in Figure 4, the load maximum error is ± 0.01 for Figure 4a, ± 0.001 for Figure 4b. In both cases, maximum open phase error is ± 0.5 degrees, short phase error is ± 0.25 degrees. In Figure 4a, the color of the residual source match curves are yellow during the first sweep. In the second sweep, maximum errors of load, open and short are $\pm 0.01 * 0.75$, $\pm 0.5 * 0.75$ degrees and $\pm 0.25 * 0.75$ respectively. The color of the curves are green in this case. And the 0.75 factors are changed to 0.5 for the third sweep with the color red. And the color blue is used for the last sweep. The same color scheme is then repeated in generating the curves in Figure 4b where the load model is more accurate. When the figures are viewed in black and white, the color scheme chosen here becomes more of a gray scale going from light to dark gray as the color changes from yellow to blue. The smaller error in the load model has brought the residual source match lower by almost 10 dB. We will examine this effect more closely in the next case study. Approximate locations of the three characterized devices are shown on a Smith chart legend accompanying the following case studies.

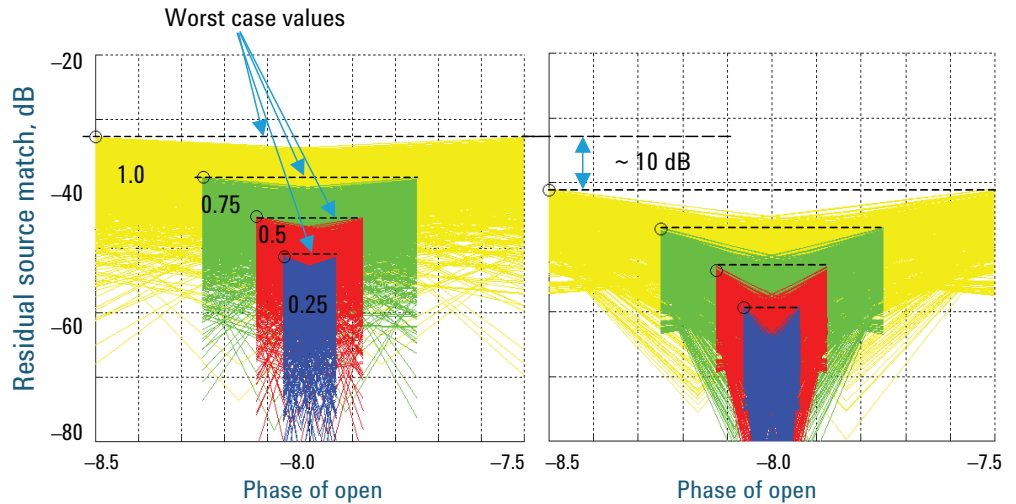


Figure 4a. Load error = ± 0.01

Figure 4b. Load error = ± 0.001

Worst case value, indicated by the dotted lines in Figures 4a and 4b, can be found for the residual source match for each of the 4 different values of the percentage factor. When the factor varies from 0 to 1, worst case value in each sweep can be found and they are plotted against the normalized errors in Case Studies III and IV. The normalized error has the same value as the percentage factor and is used simultaneously for all three error vectors in a simulation where the worst case values are found for the magnitude of residual source match and directivity and for the magnitude and phase of residual tracking. It can be alternatively defined as follows:

$$\text{Normalized error} = |\Delta\Gamma_i| / \max(|\Delta\Gamma_i|), i = 1,2,3.$$

For example, let's consider the case where $\Gamma_L = 0.032$, $\Gamma_s = -1$ and $\Gamma_0 = 1$, and the error in the load model, $\max(|\Delta\Gamma_L|)$, has a value of 0.01, the error in the short model, $\max(|\Delta\Gamma_s|)$, has a value of 0.0043 or about 0.25 degree in phase, and the error in the open model, $\max(|\Delta\Gamma_0|)$, has a value of 0.0087 or 0.5 degree in phase. If the normalized error has a value of 1.0, the worst case value for each residual error are found using the above maximum values in the variation of the error vectors. If the normalized error has a value of 0.5, each of the maximum values of errors in the models are multiplied by 0.5 before the worst case values are searched.

When $\max(|\Delta\Gamma_L|)$ has a value of 0.005 instead of 0.01, the second case that was considered in case study III, a second curve is plotted against the normalized error. And when the normalized error has a value of 1.0, it corresponds to the case where $\max(|\Delta\Gamma_L|) = 0.005$, $\max(|\Delta\Gamma_s|) = 0.25$ degree in phase, $\max(|\Delta\Gamma_0|) = 0.5$ degree in phase. Values of $\max(|\Delta\Gamma_s|)$ and $\max(|\Delta\Gamma_0|)$ have not changed for the curve where $\max(|\Delta\Gamma_L|) = 0.005$. As a result, residual errors at normalized error of 1.0 can be used directly to compare the different scenarios presented in one particular case study. On the other hand, the variation of the residual error along the normalized error axis is similar to a change in the frequency of interest. When the normalized error changes from 1.0 to 0.5, all the error vectors are effectively reduced by half and we can liken this to a decrease in the operating frequency such that the errors in the models become relatively smaller. Although this is especially true for errors in model data of the open and the short, errors in model data for a load may not have this trend.

Case III: Sensitivity of Error in Load Model

$\Gamma_s = -1$, $\max(|\Delta\Gamma_s|) = 0.0043$ or 0.25 degree in phase. $\Gamma_0 = 1$, $\max(|\Delta\Gamma_0|) = 0.0087$ or 0.5 degree in phase. $\Gamma_L = 0.032$.
 Four different values of $\max(|\Delta\Gamma_L|)$, 0.01, 0.005, 0.0025 or 0.00125.

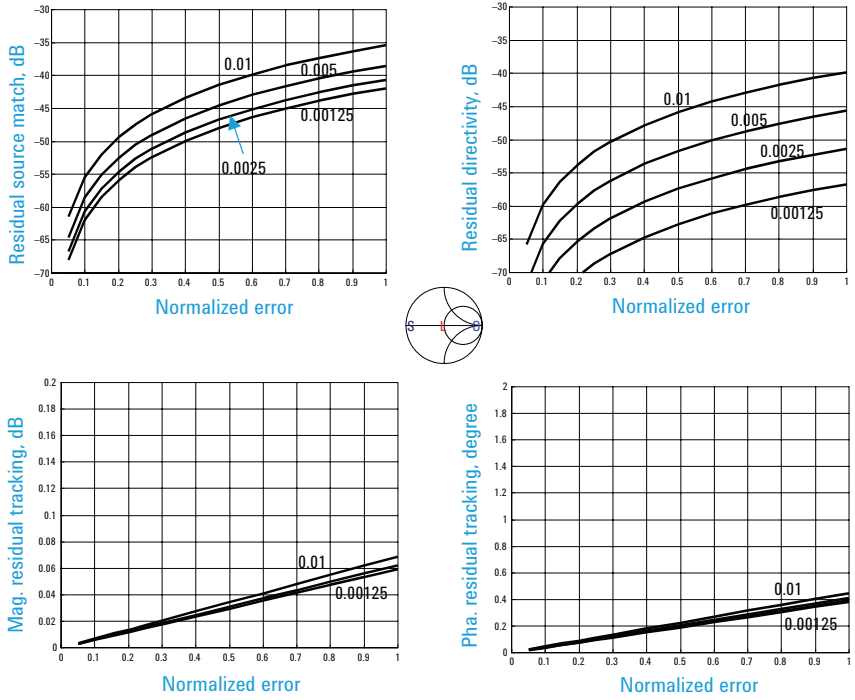


Figure 5. Sensitivity of error in model data used for the load. Four different values of $\max(|\Delta\Gamma_L|)$, 0.01, 0.005, 0.0025 or 0.00125 are considered.

A 6 dB improvement in characterizing the load reduces the residual directivity from -40 to -46 dB. It also leads to a 3 dB improvement in residual source match from -35 to -38 dB. Similar improvement in characterizing the load will continue to improve residual directivity and, to a lesser extent, residual source match. Since the error in the load model is a random number fluctuating around zero as frequency varies, one can expect the residual source match and directivity to exhibit a ripple because of this.

Case IV: Sensitivity of Error in Open Model

$\Gamma_L = 0.032$, $\max(|\Delta\Gamma_L|) = 0.01$. $\Gamma_S = -1$, $\max(|\Delta\Gamma_S|) = 0.0043$ or 0.25 degree in phase. $\Gamma_0 = 1$.

Five different values of $\max(|\Delta\Gamma_0|)$ in terms of degrees in phase, 2.0, 1.0, 0.5, 0.25, 0.125.

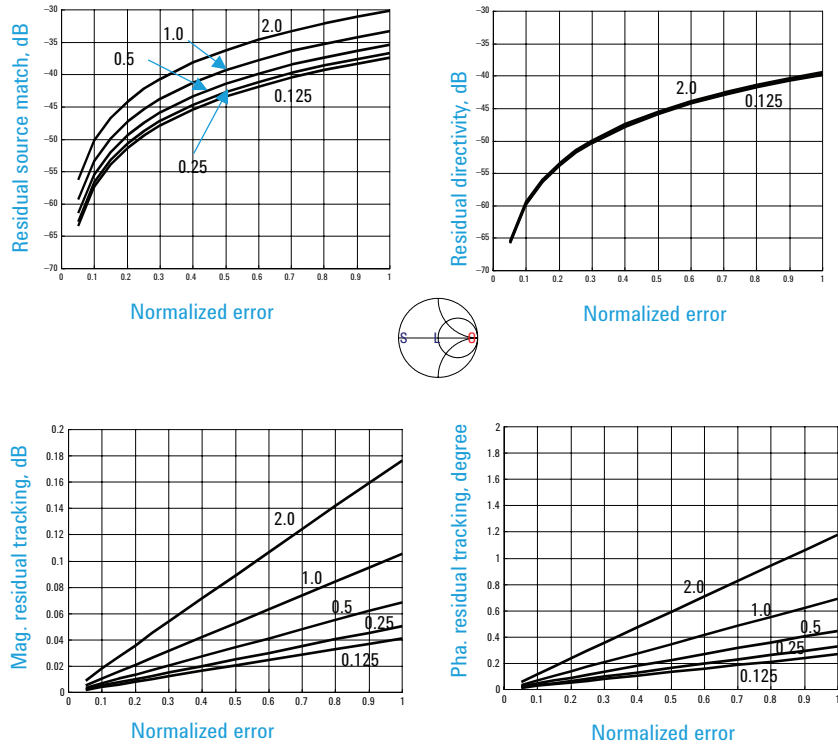


Figure 6. Sensitivity of error in model data used for the open. Five different values of $\max(|\Delta\Gamma_0|)$, in terms of degrees in phase, 2.0, 1.0, 0.5, 0.25, 0.125, are considered.

Error in open model has negligible effect on residual directivity. Its effects on residual source match and tracking diminish rapidly below errors ± 0.5 degrees phase variation. That is, unless the errors in the load model and the short model are reduced at the same time, it is not useful to measure the open to any better accuracy.

Conclusion

In this paper, we presented a study on the sensitivity of characterized device calibration technique with respect to the characterization accuracy of its devices. It is found that the *residual source match* of a characterized device calibration can be significantly affected by the accuracy of the model data for the matched load. This result underlines the importance of creating an accurate set of data for the load. A sliding termination can emulate the performance of a high quality matched load when the uniformity of the sliding section is taken into account in its measurement. In a characterized device calibration where a sliding termination is used instead of a regular matched load, its performance is thus expected to be more superior because of the important role of the load.

While the accuracy of model data for the load can improve the calibration in terms of both residual directivity and residual source match, it is interesting to find that the accuracy of model data for the open does not seem to have similar importance on the residual source match and has almost no effect on residual directivity. However, it may be due to the reason that the error in model data of the short was not reduced at the same time. Further research is warranted in this area.

Acknowledgment

The author is grateful to Mr. Ken Wong and Mr. Bryan Lai for their helpful discussions and comments on various aspects of the work presented here.

References

1. N.R. Franzen, R.A. Speciale, *A New Procedure for System Calibration and Error Removal in Automated S-parameter Measurements*, Proc. 5th European Microwave Conference (Hamburg), 1975, pp.69-73.
2. R.W. Beatty, *Invariance of the Cross Ratio Applied to Microwave Network Analysis*, National Bureau of Standards Technical Note 623, September 1972.
3. D.K. Rytting, *Improved RF Hardware and Calibration Methods for Network Analyzers*, Symposium presentation slides.
4. K. Wong, *Unknown Thru Cal*, Test Support Document, Agilent Technologies, Mar 2001.



myAgilent

www.agilent.com/find/myagilent

A personalized view into the information most relevant to you.

For more information on Agilent Technologies' products, applications or services, please contact your local Agilent office. The complete list is available at:

www.agilent.com/find/contactus

Americas

Canada	(877) 894 4414
Brazil	(11) 4197 3600
Mexico	01800 5064 800
United States	(800) 829 4444

Asia Pacific

Australia	1 800 629 485
China	800 810 0189
Hong Kong	800 938 693
India	1 800 112 929
Japan	0120 (421) 345
Korea	080 769 0800
Malaysia	1 800 888 848
Singapore	1 800 375 8100
Taiwan	0800 047 866
Other AP Countries	(65) 375 8100

Europe & Middle East

Belgium	32 (0) 2 404 93 40
Denmark	45 45 80 12 15
Finland	358 (0) 10 855 2100
France	0825 010 700*
	*0.125 €/minute
Germany	49 (0) 7031 464 6333
Ireland	1890 924 204
Israel	972-3-9288-504/544
Italy	39 02 92 60 8484
Netherlands	31 (0) 20 547 2111
Spain	34 (91) 631 3300
Sweden	0200-88 22 55
United Kingdom	44 (0) 118 927 6201

For other unlisted countries:

www.agilent.com/find/contactus

Revised: October 11, 2012

Product specifications and descriptions in this document subject to change without notice.

© Agilent Technologies, Inc. 2012
Published in USA, October 14, 2012
5991-1272EN

